Image-rotating cavity designs for improved beam quality in nanosecond optical parametric oscillators

Arlee V. Smith

Department 1118, Lasers, Optics and Remote Sensing, Sandia National Laboratories, Albuquerque, New Mexico 87185-1423

Mark S. Bowers

Aculight Corporation, Suite 113, 11805 North Creek Parkway South, Bothell, Washington 98011

Received July 11, 2000; revised manuscript received December 9, 2000

We show by computer simulation that high beam quality can be achieved in high-energy, nanosecond optical parametric oscillators by use of image-rotating resonators. Lateral walk-off between the signal and the idler beams in a nonlinear crystal creates correlations across the beams in the walk off direction, or equivalently, creates a restricted acceptance angle. These correlations can improve the beam quality in the walk-off plane. We show that image rotation or reflection can be used to improve beam quality in both planes. The lateral walk-off can be due to birefringent walk-off in type II mixing or to noncollinear mixing in type I or type II mixing.

OCIS codes: 190.497, 190.4420, 230.4320.

1. INTRODUCTION

One of the greatest challenges in scaling nanosecond optical parametric oscillators (OPO's) to high energy is obtaining good beam quality along with high efficiency. Because of constraints imposed by crystal nonlinearities and damage thresholds, scaling an OPO from low to high energy implies increasing the beam diameters while keeping the fluences, crystal lengths, and cavity length relatively unchanged. The result is a high-Fresnel-number cavity ($N_F = d^2/\lambda L$, where d is the beam diameter and L is the cavity length) that can support many transverse modes, often resulting in poor beam quality. In this paper we use a numerical model to examine the effectiveness of various image-rotating resonator designs in improving signal and idler beam quality for high-energy, nanosecond OPO's.

Beams from OPO's with small Fresnel numbers are often nearly diffraction limited because diffraction couples all transverse regions of the beams. However, as the beam diameters are increased to large Fresnel numbers, different portions of the beams uncouple and develop more-or-less independently of one another in cavities with flat mirrors. Thus uncorrelated phase and amplitude variations occur across the beam profile, resulting in poor beam quality. To improve the beam quality we must force all regions of the signal or the idler beams or both to communicate in a way that establishes more nearly uniform phase and amplitude across the beams. One way to do this is to use a confocal unstable resonator such as that shown in Fig. 1.[1–6] Light originally oscillating near the cavity axis gradually spreads over the entire beam diameter by diffraction and cavity magnification. Light is also continuously lost from the edges of the gain region for the same reasons, so after a few round trips of the cavity all the resonated light has a common ancestry and, for proper cavity alignment, a common phase. Another way to communicate phase across the beam is by spatial walk-off between the signal and the idler beams, combined with image rotations. Walk-off tends to smooth the phase of the signal beam over regions that interact with a particular portion of the idler beam. For a single pass through a crystal this part of the idler beam is a stripe of length equal to the walk-off displacement within the crystal. Over successive passes of an OPO cavity such as that shown in Fig. 1 the stripe lengthens by this amount on each pass. Without image rotation this lengthening leads to a set of stripes of uniform phase that is oriented parallel to the walk-off direction but with an independent phase for each stripe. By rotating the image 90° on each cavity pass, one can induce a uniform phase across the entire beam. For this method to work, the signal and the idler waves must have nonparallel Poynting vectors in the crystal. This is true for type II mixing with collinear pumping, but one can easily achieve the same result for type I mixing as well by tilting the pump beam relative to the cavity axis.

In this study of beam quality we use the numerical model for monochromatic OPO's described in an earlier paper.[7] We demonstrated that this model accurately predicts beam quality for a low-Fresnel-number, three-mirror-ring KTP OPO for pump levels of 2.5 times threshold and values of M^2 of at least 4. The model includes diffraction and birefringent walk-off but not group-velocity effects. The input pump and signal waves are assumed to be perfect spatial Gaussian beams. We believe that the fact that the initial signal beam is a perfect

0740-3224/2001/050706-08$15.00

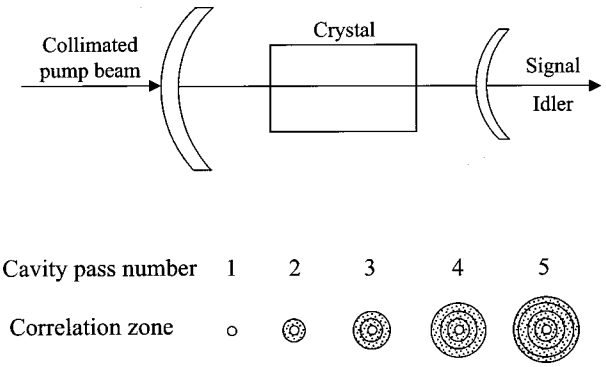

Fig. 1. Diagram of a confocal unstable resonator. The focal points of the input and output mirrors coincide. Beams are collimated on the forward pass and expand on the backward pass. The expanding zones of correlation for the signal wave after successive cavity passes are shown at the bottom of this figure, illustrating their growth about the cavity axis.

Gaussian does not invalidate the model for the purpose of beam-quality studies because in the amplification process the beam is greatly gain narrowed as a result of the nonuniform pump profile. The signal wave reaches threshold first at the center of the pump beam, so at the time of turn-on it has a small diameter and thus populates many transverse plane-wave components. Additionally, after turn on, backconversion of signal and idler to pump depletes the centers of the signal and idler beams, further populating high-order transverse components. Beam clean-up must thus occur after turn-on, so the starting profile is relatively unimportant.

The cases that we present here represent a compromise between low-Fresnel-number cavities, for which diffraction alone will produce good-quality beams, and high-Fresnel-number cavities that demand fine transverse grids for accurate modeling and thus have long computation times. At intermediate Fresnel numbers, poor beam quality is still permitted by the model, so it is meaningful to draw conclusions about whether a particular cavity design gives good-quality beams.

2. RESONATOR DESIGN STUDY

Image-rotating cavities have long been used to improve the beam quality of lasers.[8] On successive passes each portion of the laser beam samples different gain regions, averaging to some extent the gain and refractive-index inhomogeneities. This mechanism can also be effective in OPO's in which inhomogeneities of the pump light can be averaged. However, the clean-up mechanism in the OPO's modeled here is not gain averaging but the establishment of phase and amplitude correlations across the signal and idler beams owing to lateral walk-off between them as they propagate through the crystal. For type II mixing, the birefringent walk-off in a single pass of a critically phase-matched crystal is typically 0.1–1 mm. This region can be a significant fraction of the beam diameter. By its nature, parametric gain tends to establish local phase and amplitude correlations between signal and idler beams, and also within the signal beam and within the idler beam, over stripes of length equal to the walk-off and oriented parallel to walk-off. Over multiple passes through the OPO cavity these stripes can grow to cover the full signal and idler beam widths. A consequence of this correlation is that the beam divergence in the walk-off direction can be restricted to near the diffraction limit, whereas the divergence in the other direction is less restricted. This effect is often somewhat obscurely referred to as a restricted crystal acceptance angle, and it is usually analyzed in terms of tilted plane waves. The analysis presented here in terms of correlation zones is equivalent to that for tilted plane waves for monochromatic operation but is easier to visualize and apply.[9,10]

An example of divergence asymmetry may be seen in Fig. 2(b), where we show a model-generated far-field signal fluence for the simple ring OPO of Fig. 2(a). This OPO has a single crystal with walk-off between signal and idler in the $\hat{x}$ direction, as indicated by the arrow on the crystal. The ring cavity lies in the $\hat{x}$–$\hat{z}$ plane and inverts the resonated signal beam in the $\hat{x}$ dimension on each pass. The idler and pump are not resonated. Details of the modeled OPO are listed in Table 1. The Fresnel number is ~35 here and in all the cases described in this paper, and all the OPO's are pumped with 0.1-J of energy-which is ~2 times threshold. As expected, correlations in the signal beam develop over many passes as stripes in the $\hat{x}$ direction, leading to reduced divergence in that direction. Correlation between stripes is weak, however, because diffractive coupling is weak for separations greater than ~0.5 mm in the $\hat{y}$ direction. This decoupling length is considerably less than the 1.9-mm pump diameter, so the divergence in the $\hat{y}$ direction is relatively large. In contrast to the far-field fluence of Fig. 2(b), the near-field signal fluence at the output mirror is nearly symmetric in the $\hat{x}$ and $\hat{y}$ directions. Figure 3 shows sig-

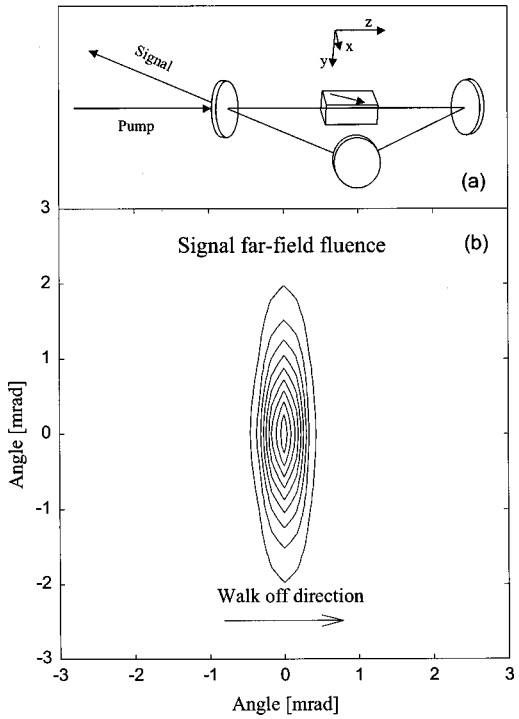

Fig. 2. (a) Simple planar ring OPO design. The walk-off between the signal and the idler beams, indicated by the arrow on the crystal, is in the plane of the ring. (b) Computed far-field signal fluence with the operating parameters of Table 1.

Table 1. Ring OPO Parameters

Parameter	Signal	Idler	Pump
Wavelength (nm)	1700	2844	1064
Refractive index	1.774	1.808	1.787
Input power–energy	1×10^{-9} W	0	0.1 J
Pulse duration (ns)	cw		7
Beam diameter FWHM (mm)	1.9(seed)		1.9
Walk-off angle (mrad)	0	36	0
Left mirror reflectivity	0.5	0	0
Other mirror reflectivities	1	1	1
Crystal length (mm)	30		
Cavity length (mm)	67		
d_{eff} (pm/V)	2		

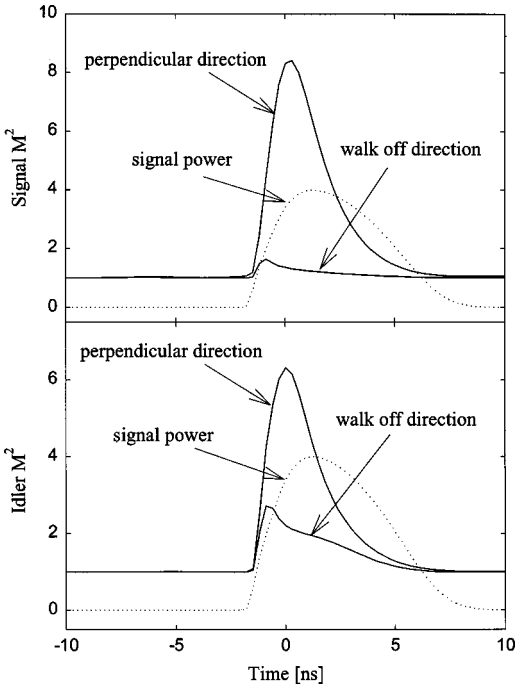

Fig. 3. (a) Signal and (b) idler beam quality as a function of time for the OPO of Fig. 2(a). Dotted curves, signal power in arbitrary units, shown for reference.

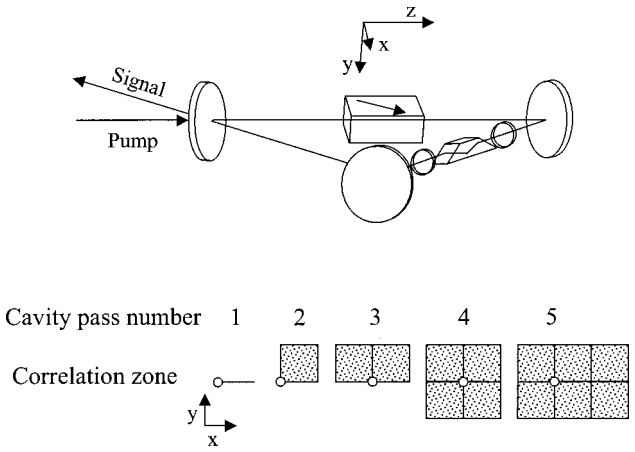

Fig. 4. Image-rotating OPO cavity design based on a dove prism image rotator. Half-wave plates before and after the dove prism rotate the signal polarization by 45°. The expanding zones of correlation for the signal wave after successive crystal passes are shown at the bottom.

nal and idler M^2 for this OPO as functions of time. For reference we have also plotted normalized signal power as dotted lines.

Of course, M^2 is not always a relevant indicator of the usefulness of a beam because it is a measure of beam distortion after tilt and first-order curvature have been removed. A beam can have a low M^2 even though the far-field distribution might vary in time owing to time-dependent tilts and curvature. However, we have found that this variance is not a serious problem with the cases presented here, so both the far-field fluence profile and the time-dependent M^2 values give useful indications of the beam quality. As we noted above, even though our model starts with a diffraction-limited signal wave, spatial gain narrowing induced by the Gaussian pump profile plus backconversion distorts the signal beam, introducing high spatial frequencies, or, equivalently, populating many highly tilted signal plane waves. This distortion causes the relatively poor signal–idler beam quality when the OPO first turns on, as shown in Fig. 3. Beam quality improves over successive cavity passes. Improvement in the walk-off direction is faster than in the orthogonal direction because walk-off is much more effective at creating correlations than is diffraction in this case.

If the image of the resonated signal wave is rotated 90° on each cavity pass, the correlation zone can extend in both transverse dimensions, leading to improved beam quality in both dimensions. Figure 4 shows one example of an image-rotating cavity, along with a diagram of the correlation zones for successive passes. A dove prism in the return leg, rotated 45° relative to the ring plane, rotates the signal beam by 90° on each pass. Wave plates before and after the prism align the signal beam polarization to an eigenpolarization of the dove prism to prevent depolarization. In the diagrams of the correlation zones at the bottom of the figure we show how the signal field initially at the origin develops zones connected by idler walk-off and image rotation. An open circle indicates an origin or a beam center. After the first pass through the crystal, a correlation zone is created that extends in the $\hat{x}$, or walk-off, direction, a distance that is equal to the single-pass idler walk-off, ρL_{crystal}. Here ρ is the angle between signal and idler Poynting vectors in the crystal, whether it is due to birefringence or to noncollinear pumping. This is shown in the figure for cavity pass number 1. This line is rotated counterclockwise by 90° in

the cavity so on the next pass through the crystal the walk-off again creates correlations in the $\hat{x}$ direction, as shown for correlation pass number 2. Repetition of the counterclockwise rotation plus walk-off on successive crystal passes creates the growing correlation zones diagrammed. In Fig. 5 we display the nearly symmetric far-field signal fluence computed for this device, again using the operating parameters of Table 1. In Fig. 6 we show

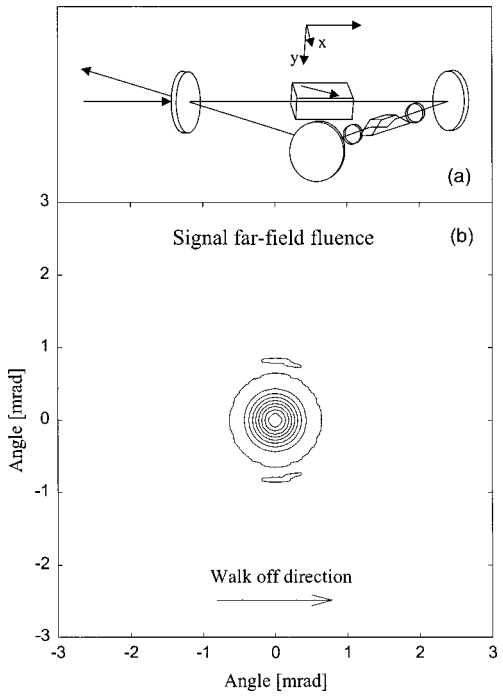

Fig. 5. (b) Far-field signal fluence for the cavity of (a) and the operating parameters of Table 1.

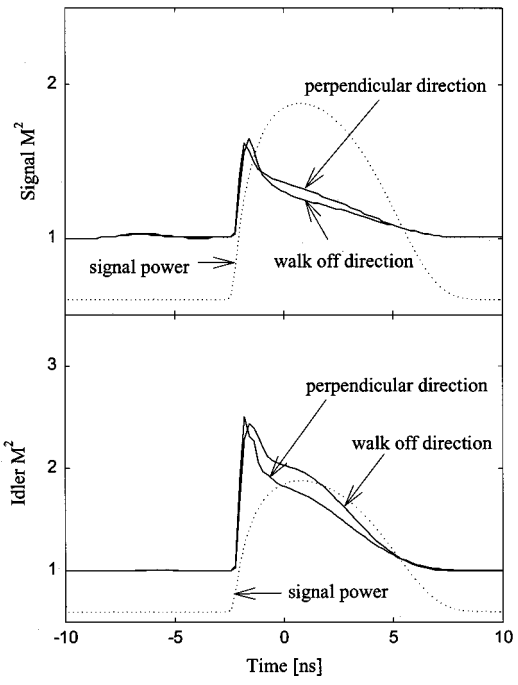

Fig. 6. (a) Signal and (b) idler beam quality as a function of time for the OPO of Fig. 5(a). Dotted curves, signal power in arbitrary units, shown for reference.

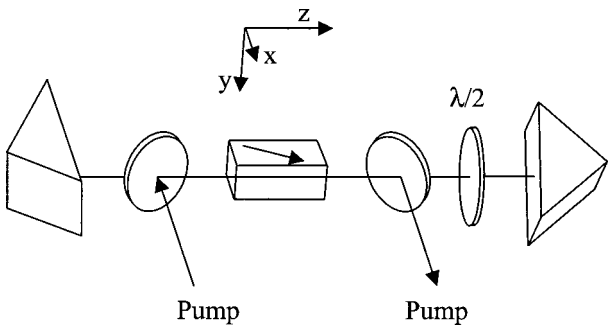

Fig. 7. Image-rotating OPO cavity design based on rotated roof prisms. The wave plate rotates the signal polarization by 45°. The pump can be coupled by use of intracavity mirrors that pass the signal and reflect the pump. Signal output coupling could be accomplished through frustrated reflection at one of the prisms, or a prism could be replaced with partially reflecting mirrors in a rooftop configuration.

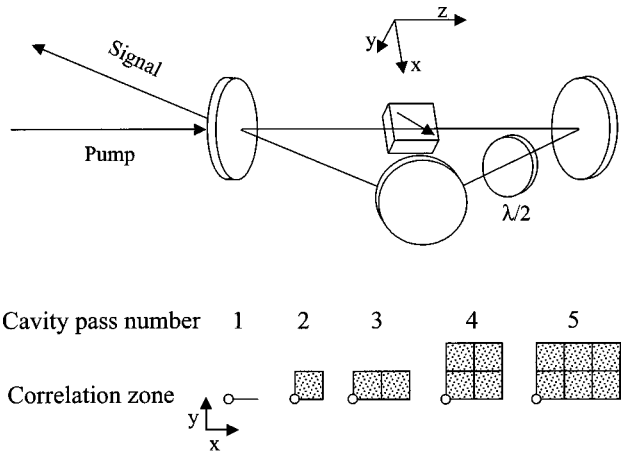

Fig. 8. Cavity design for a crystal oriented for walk-off in a plane rotated 45° relative to the plane of the cavity. The expanding zones of correlation for the signal wave after successive crystal passes are shown at the bottom, demonstrating their asymmetric growth with respect to the origin.

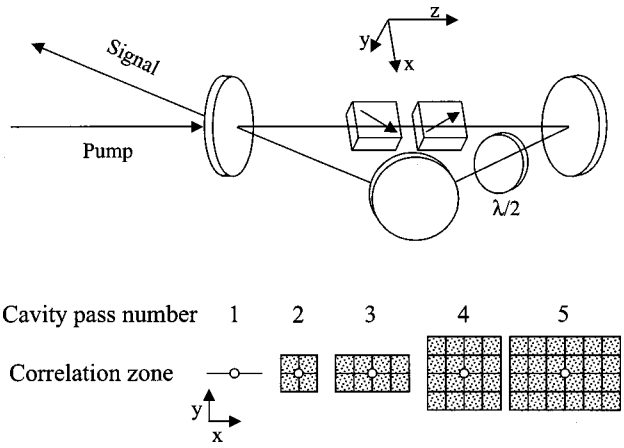

Fig. 9. Cavity design for two walk-off-compensating crystals oriented with walk-off in a plane rotated 45° relative to the plane of the cavity. The expanding zones of correlation for the signal wave after successive crystal passes are shown at the bottom, demonstrating their symmetric growth.

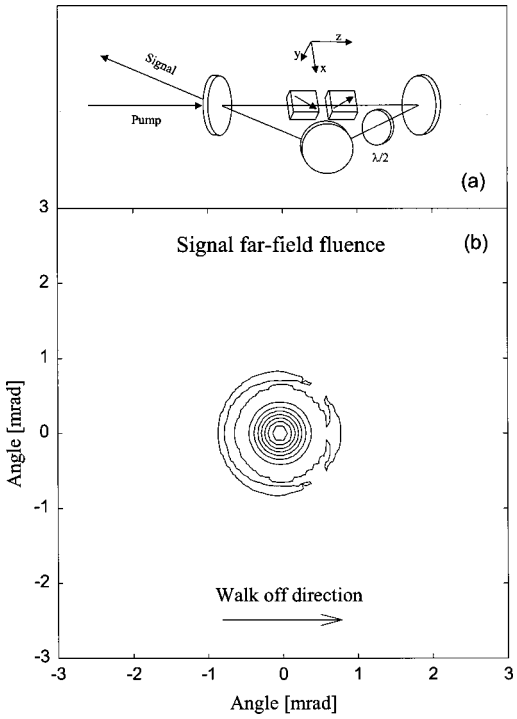

Fig. 10. (b) Far-field signal fluence for the cavity of (a) and the operating parameters of Table 1.

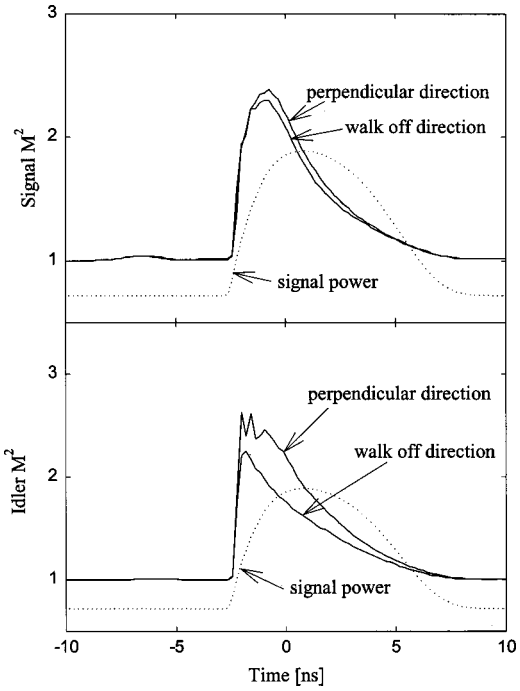

Fig. 11. (a) Signal and (b) idler beam quality as a function of time for the OPO of Fig. 10(a). Dotted curves, signal power in arbitrary units, shown for reference.

the corresponding values of M^2, along with the reference normalized signal power. The effectiveness of image rotation is apparent both in the far-field fluence pattern and in the low values for the signal M^2 in both directions. The idler beam's quality is quite good as well. The near-field irradiance profiles of the signal and the idler beams approach top-hat rather than lowest-order-Gaussian shapes, so, even though the phases are nearly flat across signal and idler beams, their values of M^2 are slightly greater than 1.

Other cavity configurations can accomplish similar image rotation. Figure 7 shows one such design based on two roof prisms, or their mirror equivalents, with a relative 45° twist about the cavity axis. For a single pass of the pump and idler waves, this design is equivalent to the dove prism design. According to our model this design also works well if the pump beam is retroreflected for a double pass of the crystal and the idler is rejected after each pass of the crystal.

Although we have shown that the image-rotating cavity is effective in generating improved beam quality, it can be somewhat awkward to implement. Imposing correlations across the beam face can also be accomplished with an image reflection in the line $x = y$. One can achieve this reflection by positioning the cavity in the plane parallel to the line $x = -y$, as shown in Fig. 8. The correlation zone develops as shown in the figure. However, this device performs poorly in our model. The output signal and idler beams tilt away from the cavity axis, and the conversion efficiency is low, similarly to the tilts and poor seeding performance observed for OPO's

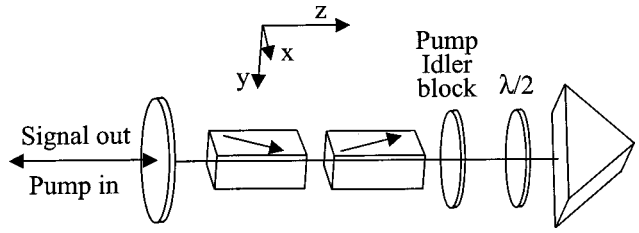

Fig. 12. Standing-wave equivalent of the ring OPO diagrammed in Fig. 10(a).

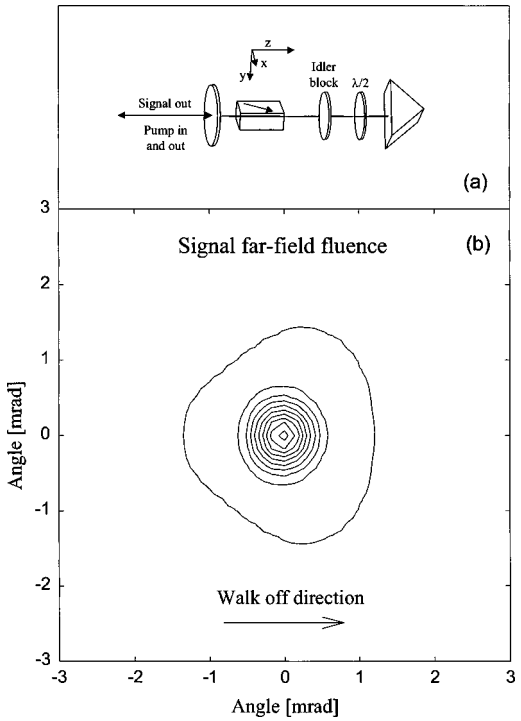

Fig. 13. (b) Far-field signal fluence for the cavity of (a) and operating parameters of Table 1.

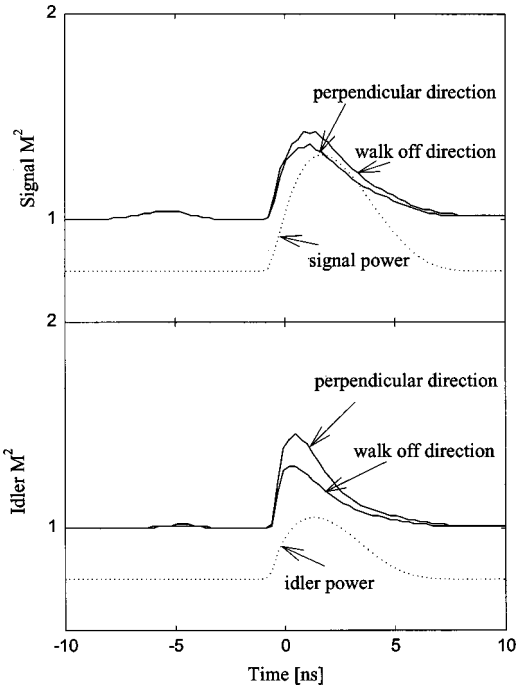

Fig. 14. (a) Signal and (b) idler beam quality as a function of time for the OPO of Fig. 13(a). Dotted curves, signal power in arbitrary units, shown for reference.

with uncompensated walk-off between signal and idler beams noted in earlier papers.[9,11,12] We showed[9] that this problem is a consequence of non-parallel signal and idler Poynting vectors in the crystal and is directly associated with the asymmetry of the correlation zones seen in Fig. 8. Based on our modeling results for many cavity designs, we believe that we can make the general claim that designs for which the correlation zones are asymmetric with respect to the origin perform poorly and should be avoided. However, if the single crystal in Fig. 8 is replaced by two walk-off-compensating crystals, as shown in Fig. 9, the correlation zone becomes symmetric, and our model predicts good performance. Figures 10 and 11 show simulations of this two-crystal design, again for the operating parameters of Table 1. The beam quality is good, although not quite so good as for a rotated beam. One disadvantage of two-crystal designs is that one cannot easily adjust the walk-off between the signal and the idler by tilting the pump beam, unlike for a single-crystal OPO, so two-crystal designs are best suited to type II interactions.

An equivalent two-crystal design can also be implemented in the standing-wave cavity shown in Fig. 12. A roof prism tilted 45° relative to the walk-off plane inverts the signal beam about the line $x = -y$. The half-wave plate rotates the signal polarization to the prism eigenpolarization and back. The pump and the idler are dumped or blocked at the right end of the cavity, and the signal exits through the left mirror. Setting the crystal and cavity lengths equal to those of the two-crystal ring design (see Table 1) gives similar efficiency and beam quality, although the idler is now computed at the right end and the signal at the left. If the pump is single passed and a single crystal is substituted for the dual crystals, the correlation zone is asymmetric, and performance is poor. However, if the pump is double passed through a single crystal, the zone is symmetric and gives the good performance shown in Figs. 13 and 14. Because the pump is double passed, we halved the crystal length here, keeping the overall cavity length the same as in Table 1. Nabors and Frangineas[13,14] demonstrated a similar design for a type I β-barium borate OPO. They tilted the

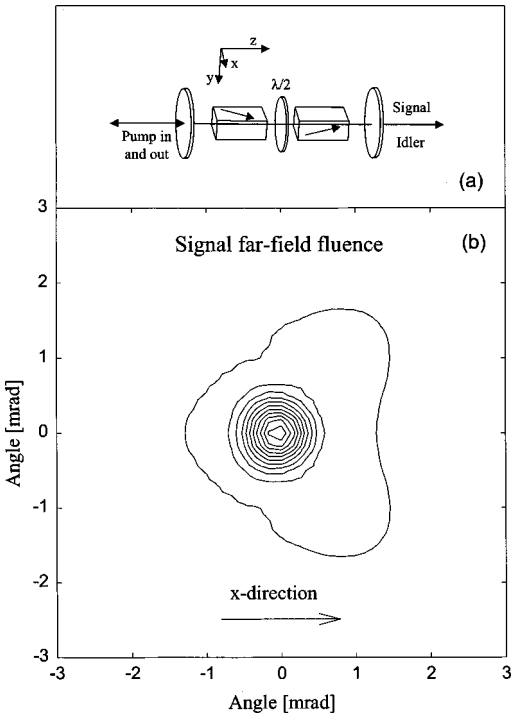

Fig. 15. (b) Far-field signal fluence for the cavity of (a) and operating parameters of Table 1.

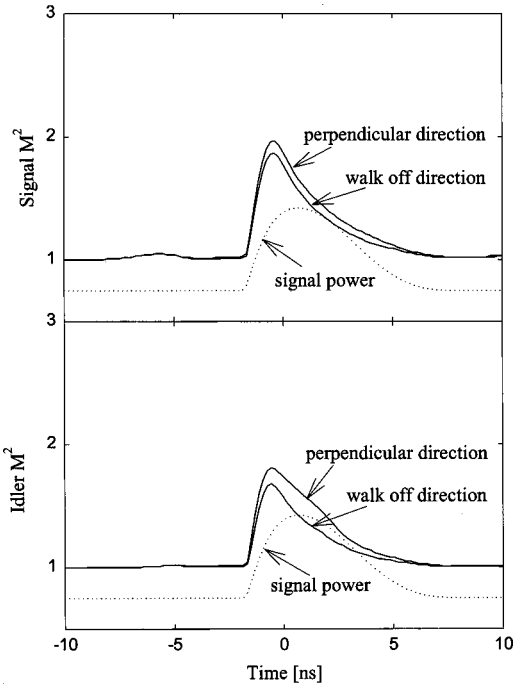

Fig. 16. (a) Signal and (b) idler beam quality as a function of time for the OPO of Fig. 15(a). Dotted curves, signal power in arbitrary units, shown for reference.

pump wave along $\hat{x} + \hat{y}$ to create idler walk-off in that direction. The prism was oriented to reverse the beam in the $\hat{x}$ direction, and the wave plate was eliminated. They measured an order-of-magnitude reduction in M^2 relative to collinear pumping for OPO's pumped by 100 mJ of 355-nm light in 3-ns pulses. Recently Anstett *et al.*[15] demonstrated the device of Fig. 13, using a 70-mJ, 355-nm pump with a diameter of 4.5 mm and a type II β-barium borate crystal in a 6-mm-long cavity. They report a factor-of-4 reduction in the signal M^2 in the nonwalk-off direction while good beam quality was maintained in the walk-off direction. Both of these laboratory OPO's are broadband, indicating that our monochromatic model is useful in predicting beam quality for multilongitudinal-mode as well as single-longitudinal-mode OPO's.

Another method of creating two-dimensional correlation zones is to use two crystals in a standing-wave cavity oriented such that walk-off in the first is in the $\hat{x}$ direction and in the second is in the $\hat{y}$ direction. If the pump is double passed, this design also gives symmetric correlation zones. Model results for this are shown in Figs. 15 and 16. We find that the beam quality is good for both signal and idler. The intercrystal wave plate rotates the polarization of all three waves by 90°.

Undoubtedly other designs that give symmetric correlation zones are possible, but we hope that by showing these examples we illustrate the benefits of such designs and of our method of analysis, which should simplify the design process. The examples that we presented here all used 100 mJ of pump light. However, we scaled the energy to 1 J with enlarged beam diameters and found that for those designs that generate high-quality beams the model still works well. For designs associated with poor beam quality, the beams develop too much spatial structure to be accurately modeled with our limited computational power. Of course these designs are not of much practical interest anyway because of their poor beam quality, so our model is useful even for OPO's operating at energies of 1 J and higher.

3. CONCLUSIONS

We have shown that for a class of singly resonant OPO cavity designs the generated signal and idler beams can be of high quality with nearly circular far-field distributions, and the efficiency can be high. These are resonators that use Poynting vector walk-off between the signal and the idler beams to create symmetric, two-dimensional correlation zones through beam rotation about the signal beam axis, or through beam reflection in a diagonal line $x = y$, or through use of two crystals with walk-off in orthogonal directions. If the correlation zones are not symmetric about the cavity axis our model predicts poor efficiency and tilted beams. Two of the favored designs have been experimentally investigated[13,14] and have been shown to generate much improved beam quality relative to other designs.

We believe that the monochromatic model used in this study should apply to both monochromatic and broadband OPO's, and this assumption is supported by reports of laboratory demonstrations.[13–15] In broadband OPO's there is temporal as well as spatial walk-off, so the development of correlation zones is more complicated than for the monochromatic case. Three-dimensional rather than two-dimensional zones must be considered. From numerous experimental studies of OPO linewidth, we know that the temporal extent of the walk-off is approximately equal to the single-pass temporal walk-off between signal and idler multiplied by the number of passes during the pulse. This result implies that over this temporal zone the transverse correlations can still develop, so our model should still be quite good. A limited comparison between a broad-bandwidth model[9] and the monochromatic model supports this conclusion.

Although we have not done so, our model also makes it possible to study the influence of pump beam imperfections on signal and idler beam quality. We anticipate that cavities with true rotation rather than reflection will best average any imperfections in the amplitude and phase of the pump beam.

ACKNOWLEDGMENTS

This study was supported by the U.S. Department of Energy under contract DE-AC04-94AL85000. Sandia National Laboratory is a multiprogram laboratory operated by Sandia Corporation, a Lockheed Martin Company, for the U.S. Department of Energy.

A. V. Smith's e-mail address is arlsmit@sandia.gov.

REFERENCES

1. W. A. Neuman and S. P. Velsko, "Effect of cavity design on optical parametric oscillator performance," in *Advanced Solid-State Lasers*, S. A. Payne and C. Pollock, eds., Vol. 1 of OSA Topics in Optics and Photonics Series (Optical Society of America, Washington, D.C., 1996), pp. 179–181.
2. M. K. Brown and M. S. Bowers, "High energy, near diffraction limited output from optical parametric oscillators using unstable resonators," in *Solid State Lasers VI*, R. Scheps, ed., Proc. SPIE **2986**, 113–122 (1997).
3. J. N. Farmer, M. S. Bowers, and W. S. Scharpf, "High brightness eyesafe optical parametric oscillator using confocal unstable resonators," in *Advanced Solid-State Lasers*, M. M. Fejer, H. Injeyen, and U. Keller, eds., Vol. 26 of OSA Topics in Optics and Photonics Series (Optical Society of America, Washington, D.C., 1999), pp. 567–571.
4. T. Debuisschért, D. Mathieu, J. Raffy, L. Becouarn, E. Lallier, and J.-P. Pocholle, "High beam quality unstable cavity infrared optical parametric oscillator," in *Laser Resonators*, P. Galarneau and A. V. Kudryashov, eds., Proc. SPIE **3267**, 170–180 (1998).
5. B. C. Johnson, V. J. Newell, J. B. Clark, and E. S. McPhee, "Narrow-bandwidth low-divergence optical parametric oscillator for nonlinear frequency-conversion applications," J. Opt. Soc. Am. B **12**, 2122–2127 (1995).
6. S. Haidar and H. Ito, "Injection-seeded optical parametric oscillator for efficient difference frequency generation in mid-IR," Opt. Commun. **171**, 171–176 (1999).
7. A. V. Smith, W. J. Alford, T. D. Raymond, and M. S. Bowers, "Comparison of a numerical model with measured performance of a seeded nanosecond KTP optical parametric oscillator," J. Opt. Soc. Am. B **12**, 2253–2267 (1995).
8. Y. A. Anan'ev *Laser Resonators and Beam Divergence Problem* (Hilger, New York, 1992), pp. 321–327.
9. W. J. Alford, R. J. Gehr, R. L. Schmitt, A. V. Smith, and G. Arisholm, "Beam tilt and angular dispersion in broadbandwidth, nanosecond optical parametric oscillators," J. Opt. Soc. Am. B **16**, 1525–1532 (1999).

10. A. V. Smith, D. J. Armstrong, and W. J. Alford, "Increased acceptance bandwidths in optical frequency conversion by use of multiple walk-off-compensating nonlinear crystals," J. Opt. Soc. Am. B **15**, 122–141 (1998).
11. J. G. Haub, R. M. Hentschel, M. J. Johnson, and B. J. Orr, "Controlling the performance of a pulsed optical parametric oscillator: a survey of techniques and spectroscopic applications," J. Opt. Soc. Am. B **12**, 2128–2141 (1995).
12. R. Urschel, U. Bader, A. Borsutzky, and R. Wallenstein, "Spectral properties and conversion efficiency of 355-nm-pumped pulsed optical parametric oscillators of β-barium borate with noncollinear phase matching," J. Opt. Soc. Am. B **16**, 565–579 (1999).
13. C. D. Nabors and G. Frangineas, "Optical parametric oscillator with bi-noncollinear, porro prism cavity," in *Advanced Solid State Lasers*, C. R. Pollock and W. R. Bosenberg, eds., Vol. 10 of OSA Topics in Optics and Photonics Series (Optical Society of America, Washington, D.C., 1997), pp. 90–93.
14. C. D. Nabors and G. Frangineas, "Optical parametric oscillator with porro prism cavity," U.S. patent 5,781,571 (July 14, 1998).
15. G. Anstett, G. Goritz, D. Kabs, R. Urschel, R. Wallenstein, and A. Borsutzky, "Reduction of the spectral width and beam divergence of a BBO-OPO by using collinear type-II phase matching and backreflection of the pump beam," Appl. Phys. B (to be published).